INM RAS COUPLED ARCTIC OCEAN\SEA ICE MODEL. THE RESULTS OF THE AOMIP 31-YEAR COORDINATED SPIN-UP 1948-1978

Nikolai G. Yakovlev*
Institute of Numerical Mathematics Russian Academy of Sciences,
Moscow, Russia

1. INTRODUCTION

The development of the mathematical theory of climate and numerical methods for the climate system (atmosphere – ocean - sea ice - permafrost - land) modeling is one of the topics for the Institute of Numerical Mathematics of the Russian Academy of Sciences (INM RAS). There are Atmosphere General Circulation model (AGCM) (Atmosphere Model Intercomparison Project participant), global coupled AGCM\Ocean Global Circulation Model (OGCM) and some regional ocean\sea models were developed and used for climate studies at INM RAS. On the basis of the extended experience in 3D large-scale ocean climate modeling the new coupled ocean\sea ice model has been developed for Arctic Ocean and polar seas climate studies.

The model to the date is aimed mostly to test the numerical schemes, physical parameterization and get the experience in Arctic Ocean modeling. From this point of view this model may be called a “toy” model. Nevertheless, no doubt that this model will be further developed for higher spatial resolution, and expanded to wider area. In the future this model should be nested in the global Atmosphere-Ocean model.

The very good way of model development is the model comparison projects. Arctic Ocean Model Intercomparison Project (AOMIP), http://fish.cims.nyu.edu/~holland/project_aomip/purpose.html, is the international effort to investigate the ability of the various models to simulate the climate system of the Arctic Ocean and sea ice on the time scale of decades and on this basis to formulate the necessary improvements of the Arctic Ocean coupled models.

The Arctic Ocean models community represented now by several model pedigrees: MOM (Bryan, 1969), POM (Blumberg and Mellor, 1987) and MICOM. The community of the models represented mainly by MOM-based models with viscous-plastic rheology for sea ice. Despite various improvements and parameterizations many of the characteristics of the models of similar pedigree and close spatial resolution should not be different. In fact high sensitivity of arctic processes to model parameters leads to striking differences in model results.

The numerical basis of the model presented here is quite different from the “traditional” ocean general circulation models – MOM, POM or MICOM. This is why the participation of the model in the intercomparison projects may be very interesting and useful for understanding of the limits of the knowledge of the nature of the Arctic Ocean.

The first stage of the AOMIP is the coordinated spin-up under specified standard forcing and initial conditions. This presentation is devoted to the model description and to some preliminary results of the 1948-1978 years run with the special focus to Atlantic Water inflow simulation, ice and snow cover characteristics.

2. THE INM RAS ARCTIC MODEL

2.1 Physical Formulation

Ocean model is a hydrostatic primitive equation one, with Boussinesque and noncompressibility approximations. The surface salinity restoring procedure with the time scale of 180 days is applied at the sea surface to prevent model drift associated with the freshwater flux disbalance. This restoring is allowed by AOMIP regulations.

The upper ocean surface ζ may oscillate due to linearized kinematical condition for the vertical velocity

$$w = -\frac{\partial \zeta}{\partial t}, \quad z = 0\ . \tag{1}$$

Thus, model may take into account tidal dynamics on sufficiently deep water.

Ocean is driven by wind and ice stress, by river discharge (both mass transport and salinity flux $Q_{S,b}$

$$Q_{S,b} = -(S_0 - S)\cdot V\ , \tag{2}$$

are taken into account, but there is no heat transport, $S_0 \approx 10$ ppt for large scale model), and by mass, salt and heat transports through the open boundaries:

* * *Corresponding author address:* Nikolai G. Yakovlev, Inst. of Numerical Mathematics RAS, Gubkin 8, GSP-1 Moscow, 119991 Russia;
e-mail: iakovlev@inm.ras.ru

$$Q_T = \begin{cases} u_n T, \ \text{outflow} \ \ u_n > 0, \\ u_n T^* + \dfrac{A_T^*}{h}(T^* - T), \ \text{inflow} \ \ u_n < 0 \end{cases} \quad (3)$$

(the same formula is for the salinity fluxes).

Here T is a model temperature, T^* is an observed temperature at boundary, u_n is a velocity, normal to the boundary, A_T^* is a constant (efficient diffusion coefficient) and h is a length scale (say – grid size). Parameter $\dfrac{A_T^*}{h}$ was chosen to be equal to 30cm/s, providing relaxation time of T to T^* to be about 3 days.

The "inverted barometer" effect (direct atmosphere pressure) is also taken into account

$$P = P_a + \rho_w g \zeta \ , \ \ z = 0 \ , \quad (4)$$

P is the pressure, P_a is the atmospheric pressure at sea level surface, g - gravity acceleration.

Horizontal turbulence is approximated by simple Boussinesque approximation with harmonic friction. The special parameterization for horizontal turbulence on bottom slopes is presented in section 2.3. Bottom friction is linear with the relaxation time 4 days (Maslowski, 1996).

There is a Parkinson and Washington, 1979 style model for ice-snow thermodynamics. Atmosphere forcing of the model (shortwave and net longwave radiation, sensible and latent heat fluxes) is specified according to the AOMIP. There is no diurnal averaging of the shortwave radiation.

There are several (at the time – 8) gradations of the ice thickness, with the simple parameterization of the ice thickness redistribution during ridging (personal communication by I. Polyakov, IARC, UAF, AK). The ice redistributer conserves heat and salt content of the ice.

The heat flux from ocean to the ice bottom is described as

$$Q_w = \rho_w c_W C_{Dw} W (T_W - T_F)\ . \quad (5)$$

Here ρ_W is the density of water, c_W is the specific heat capacity of water, $W \cong 1 \div 3 cm/s$, C_{Dw} is a constant transfer coefficient. In the model $C_{Dw}W = 3.0 \cdot 10^{-3}$ (Wadhams, *et.al.*, 1979).

The freezing point of sea water is by Millero, 1978. For the wide range of salinity this equation may be approximated by linear formula

$$T_F = -0.0545 \cdot S\ . \quad (6)$$

The model takes into account the aging of snow, when snow is converted into ice with the time scale of $10^7 s$. The immediately built ice thickness during freezing conditions is 1 cm. Rain and snow fraction of precipitation are stipulated by the air temperature T_a (Weatherly and Walsh, 1996)

$$P_S = \begin{cases} 1.0 & T_a < -5^0 C \\ 1 - (T_a + 5^0 C)/10 & -5^0 C \le T \le 5^0 C \\ 0 & T_a > 5^0 C \end{cases} \quad (7)$$

The viscous-plastic rheology model ("cavitating fluid" by Flato and Hibler (1992) or elliptical by Hibler (1979)) is applied for the ice dynamics. For the elliptical rheology the formulation by Harder, 1996 is used. The ice strength parameter according to SIMIP results (Kreyshner M., 2000) is $1.5 \cdot 10^4 N \cdot m^{-2}$.

Vertical turbulence coefficients (momentum ν and temperature-salinity $\nu_{T,S}$) are parameterized by the generalized Monin-Obukhov theory (see Kowalik and Polyakov, 1999):

$$\nu = \max(1., (0.05 \cdot L)^2 \sqrt{\left(\frac{\partial u}{\partial z}\right)^2 + \left(\frac{\partial v}{\partial z}\right)^2 - K_\rho \frac{1}{\rho}\frac{\partial \rho}{\partial z}}) \ ,$$
$$L = 25\, m\ ,$$
$$K_\rho = \begin{cases} 1, \ \dfrac{\partial \rho}{\partial z} \ge 0 \\ 10^2, \dfrac{\partial \rho}{\partial z} < 0, \end{cases} \quad (8)$$
$$\nu_{T,S} = 0.1 \cdot \nu$$

The value of K_ρ for unstable stratification is tuned to describe the convection events in large-scale model.

2.2 Discrete Approximation

The model is based on the finite-element (FE) spatial approximations. The detailed description of the ocean part of the model is presented by Iakovlev, 1998.

Time approximation is made by the time-splitting scheme with some special treatment of nonlinear sea ice rheology. There the step of vertical turbulent diffusion of temperature and salinity is extracted, when snow-ice thermal evolution and vertical profiles of temperature and salinity over the whole depth are determined simultaneously by implicit time scheme. Wind drift problem is solved for water and ice current velocities in a similar way. To improve the approximation of the ice-water quadratic friction this step is run several times (2-4) with the "inner" smaller time step. At each "inner" step vertical mixture coefficients are updated. Temperature, salinity and momentum transports are approximated by the FE upwind scheme with no crosswind diffusion by Hughes and Brooks, 1979. For the ice mass and compactness transports the FE analog of the first order directed differences scheme was developed.

The high nonlinear Ice rheology is treated by explicit scheme with small “inner” time step – approximately 1 min. It is important to notice, that ice rheology is very “fast” process so it was applied twice on each time step of the model – after wind induced drift estimate and after Coriolis-sea level action.

For the illustration of the statement let the ice dynamics equations for ice drift velocity $\vec{u}_i$ be as follows:

$$\frac{\partial \vec{u}_i}{\partial t} + l\vec{k} \times \vec{u}_i + \vec{D} + \vec{S} = \vec{R} . \qquad (9)$$

Here $\vec{D}$ is the sea level gradient, $\vec{S}$ - wind stress and $\vec{R}$ is force caused by sea ice rheology, l - Coriolis parameter, $\vec{k}$ - unit vertical vector. Then the time splitting algorithm on the time interval (t_j, t_{j+1}) вmay be formulated as a sequence of problems:

1. $$\frac{\partial \vec{u}_i}{\partial t} + \vec{S} = 0, \qquad t \in (t_j, t_{j+1}) , \qquad (10)$$

with the initial condition $\vec{u}_i^{\,j}$. The result is $\vec{u}_i^{(1)}$, attributed to the moment t_j;

2. $$\frac{\partial \vec{u}_i}{\partial t} = \vec{R}, \qquad t \in (t_j, \frac{1}{2}(t_j + t_{j+1})) , \qquad (11)$$

with the initial condition $\vec{u}_i^{(1)}$. The result is $\vec{u}_i^{(2)}$, attributed to the moment t_j;

3. $$\frac{\partial \vec{u}_i}{\partial t} + l\vec{k} \times \vec{u}_i + \vec{D} = 0, \qquad t \in (t_j, t_{j+1}) , \qquad (12)$$

with the initial condition $\vec{u}_i^{(2)}$. The result is $\vec{u}_i^{(3)}$, attributed to the moment $\frac{1}{2}(t_j + t_{j+1})$;

4. $$\frac{\partial \vec{u}_i}{\partial t} = \vec{R}, \qquad t \in (\frac{1}{2}(t_j + t_{j+1}), t_{j+1}) , \qquad (13)$$

with the initial condition $\vec{u}_i^{(3)}$. The result is the approximation of the solution $\vec{u}_i^{\,j+1}$ of the problem (9) at time $t = t_{j+1}$. If $\vec{S} \equiv \vec{0}$, $l\vec{k} \times \vec{u}_i + \vec{D} \equiv \vec{0}$ we will obtain the solution of the simple problem

$$\frac{\partial \vec{u}_i}{\partial t} = \vec{R}, \qquad t \in (t_j, t_{j+1}) \qquad (14)$$

The integral function of the model is the sea level elevation, which is determined by implicit time scheme by the GMRES method. It is very important to solve the problem for the sea level ζ as accurate as possible, for sea level equation in the model is essentially the continuity equation and accuracy of ζ determines the accuracy of mass, heat and salt conservation laws.

2.3 Coastal Jets Parameterization

It is commonly accepted now that the current state of the Arctic Ocean depends significantly on the parameters of the Atlantic Water and especially on the intensive jet-like flows of AW through narrow passages. Origin of these jets and their behavior are not understood very well and low resolution models without specially formulated parameterizations are not able to reproduce major features of the AW circulation in the Arctic Ocean. Very high resolution models can solve this problem better but it takes too much computer resources.

The possible alternative to the simulation of the jets in a coarse resolution models is to take into account the “topographic stress” in a form of “Neptune effect” by Holloway (1992) (this approach was applied to Arctic Ocean by Nazarenko, *et. al*. (1998)) further developed in terms of the Maximum Entropy Production (MEP) principle by Kazantsev, et. al. (1998) with the application to the Arctic Ocean by Polyakov (2001). In the model the simplified version of the last theory was implemented. The main assumptions were that in the deep ocean Neptune forcing balances the “ordinary” horizontal turbulent viscosity and that the “Neptune” induced velocity is about 5 cm/s. In this presentation we will focus our attention on results of regular model with no topographic stress parameterization.

2.4 Model Layout

Model domain covers area north 65N. Equations are treated in rotated coordinates with the North Pole located at 0N, 180W. This version of the model is aimed mostly to test numerical schemes and physical parameterizations, so the spatial grid size is 1 deg. (approx. 111 km) in these new coordinates. Vertical resolution is 16 levels. There are 5 islands. Open boundaries are located in Norwegian Sea, in Denmark Strait, in Bering Strait and in two straits of Canadian archipelago – M’Clure and Nares.

Model bottom topography represented by Lomonosov and Mendeleev Ridges, Nansen and Canadian basins. Gakkel Ridge is not resolved in this coarse resolution model.

There were specified 8 rivers – Ob, Yenisei, Lena, McKenzie, Kolyma, Mezen, Northern Dvina and Pechora with nonzero constant discharges during May-October, Hibler and Bryan (1987).

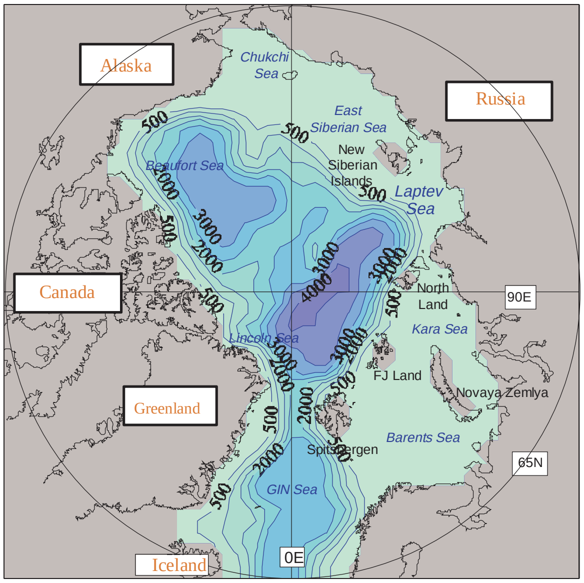

Fig.1. Model Area.

Model runs with the ”outer” time step of 1 hour. Formally model is stable for time steps as large as 12 hours, but the forcing used for the study is daily, so for the sake of approximation time step is rather small.

3. FORCING AND INITIAL CONDITIONS

3.1 Atmosphere Parameters

All the components of atmosphere forcing for the Coordinated Spin-Up case were specified to be the same for all AOMIP models (see AOMIP web site http://fish.cims.nyu.edu/~holland/project_aomip/purpose.html:

- NCEP\NCAR daily sea level atmosphere pressure;
- NCEP\NCAR daily air temperature;
- Humidity 90%;
- Monthly mean cloud cover – no spatial variations (Hushchke, 1969);
- Precipitation – corrected version by Yang, 1999.

Short wave solar radiation was with diurnal (night-day) time variability.

3.2 Ocean Parameters

In the run the PHC 2.0, Steele *et. al*., (2001) monthly mean temperature and salinity were specified as initial conditions and as boundary conditions for inflow parts of open passages. To reduce possible model drift due to inconsistency in fresh water balance there was a climate restoring to the PHC 2.0 surface salinity with a time scale of 180 days.

At open boundaries there were specified time constant mass transports. In Norwegian Sea – 8 Sv total inflow (Polyakov, 2001), with inflow along Scandinavia and outflow along Iceland, in the upper 100 m velocity 2 times larger then in deeper waters. In Bering Strait – total 0.8 Sv (Zhang, *et. al*., 1998), distributed uniformly vertically and linearwise from maximum value at Alaska to zero at Siberia. Uniform velocities were specified in all other passages with transports: 0.8 Sv – M'Clure, 0.7 Sv – Nares (Zhang, *et. al*., 1998). The mass transport in Denmark Strait was set to 7.4415 to compensate the summer river discharge (annual mean 0.1415 Sv).

3.3 Initial Conditions

Initial conditions were the PHC 2.0 January temperature and salinity, no water and ice motion, no sea level elevation. Ice thickness and compactness were 2 m and 0.9 in points with the surface temperature $T < T_F + 0.01^o C$.

4. THE 31-YEAR SPIN-UP RESULTS

4.1 Sea Level

Sea level structure (Fig. 2) exhibits several features – Transpolar drift, level rise in Beaufort Sea, West Spitsbergen and East Greenland currents, the jet, associated with the Bering Strait inflow. Total level difference between Beaufort Gyre and Norwegian Sea is about 60 cm.

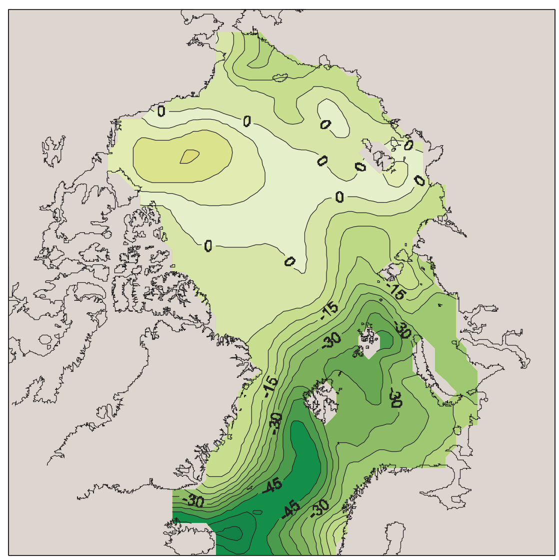

Fig. 2. Sea level (cm) for April 1978.

In September one can see the effect of river runoff and intensified Atlantic Water inflow in Barents Sea (Fig. 3)

The intensive cyclone in the Chukchi Sea is an artifact and may be attributed to inconsistency of wind pattern and specified Bering Strait mass transport.

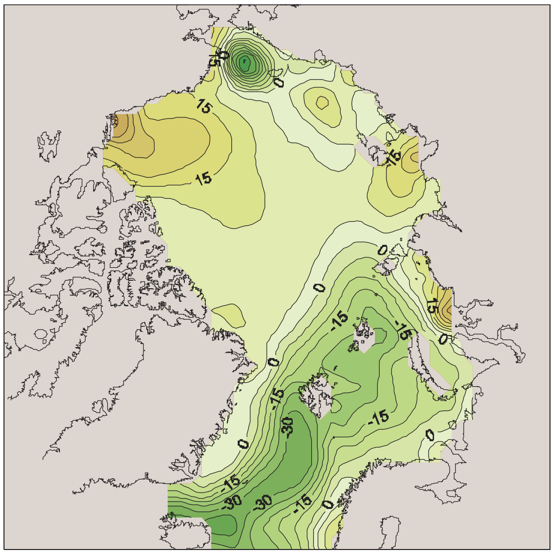

Fig. 3. Sea level (cm) for September 1978.

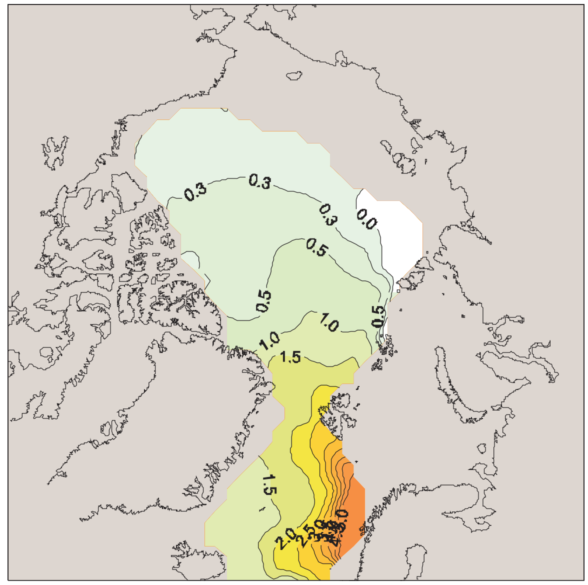

Fig. 4. Temperature (C). Atlantic water inflow at 500 m for April 1978.

4.2 Atlantic water inflow

Atlantic water (AW) inflow and propagation supposed to be one of the kernel mechanisms of the Arctic Ocean climate formation and variability. AW is the only significant source of heat during winter, possibly preventing Arctic from the overcooling and formation of thick ice. The problem is that the volume of observations is not sufficient to derive the general scheme of the AW propagation on the quantitative basis. Investigation of the AW fate in the Arctic by models is limited by the models ability to reproduce the AW transport by (probably) very narrow jets. The physical nature of the circulation in the AW layer (~500m) is also under discussion. The reproduction of the complicated 3D circulation in the 400 km wide Fram Strait is a great challenge for a coarse and medium resolution models from the numerical point of view as well.

The results of the spin-up show that at the depth of 500 m AW enters Arctic mostly with the West Spitsbergen current. There is no southward East Greenland current (EGC) at the depth, one may even detect "anti" EGC along the Greenland continental slope. In the temperature distribution (fig. 4) one may detect the trace of the coastal jet, transporting warm water toward Laptev Sea. In the Central Arctic temperature distribution is rather simple, with just a slight influence of bottom topography.

In the velocity at the 500 m depth there is a comparatively intensive West Spitsbergen current with velocities up to 8 cm/s. This jet goes further along the continental slope and dissipates in the Northern Laptev Sea. In the Central Arctic velocity is represented by cyclonic gyre above Makarov basin, with a jet approximately attached to Lomonosov Ridge (velocities about 1cm/s). In the Beaufort Sea there is a weak anticyclonic gyre.

According to the velocity field AW may penetrate Arctic three ways: along Eurasian continental slope, along Greenland slope and above Lomonosov Ridge.

The vertical sections of the Fram Strait are presented on fig. 6 (temperature) and 7 (velocity). The warm core of the AW is located at 700 m depth and shifted to the Spitsbergen. The layer of the water with temperature above +1C is between 500 and 1300 m depth.

Velocity section exhibits complicated layered structure. West Spitsbergen current occupies all the slope area from the surface to the 1400 m depth. Off the WSC zone there are 3 layers of water outflow. The velocity in the middle zone is up to 2 cm/s. The southward East Greenland current is located in upper 200 m layer only.

The time series of the mean temperature in the AW layer (450-1500 m) is presented on fig. 8. It is clear that model dissipates the AW temperature and reaches slow evolution with the temperature scale of $2.5\cdot10^{-3}$ (initial value $2.2\cdot10^{-2}$) in 15-20 years.

4.3 Sea Ice and Snow

Ice and snow characteristics are not the primary goal of the AOMIP at the date. Nevertheless ice\snow cover state is of great importance for adjacent applications and, partly, may be a measure of a model quality and a realism of the parameter choice.

Time series of the ice cover area and ice extent are presented on Fig. 9. Area assumed to be covered by ice if total ice compactness over all thickness gradations is more then 0.1. Here we can see that time scale of the ice spin-up in a coupled model –

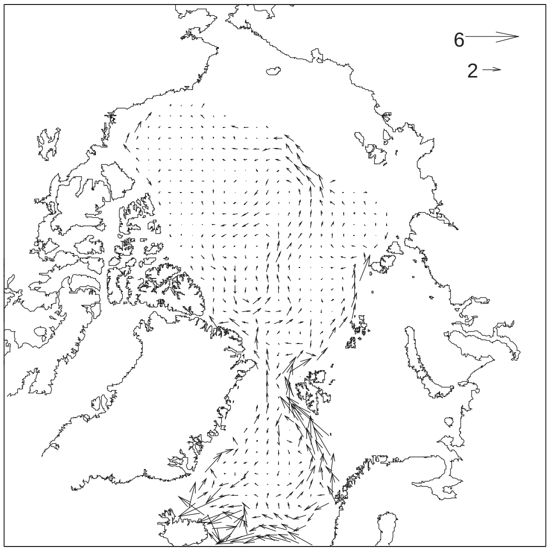

Fig. 5. Atlantic water layer velocities at 500 m for April 1978.

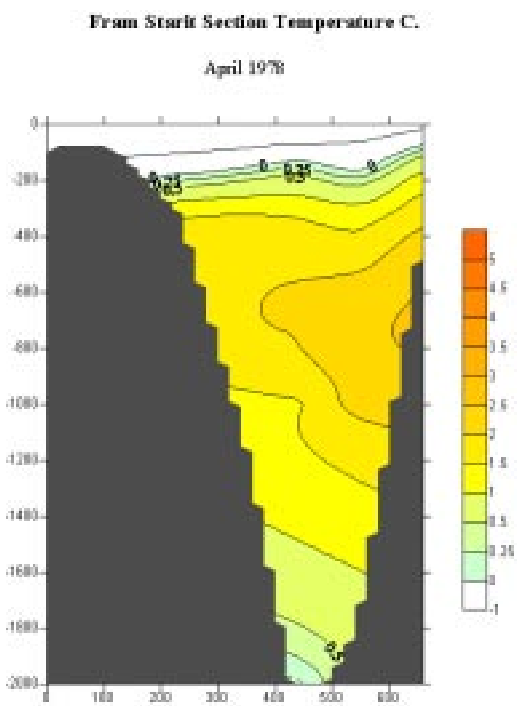

Fig. 6. Fram Strait Section. Temperature. Greenland is to the left.

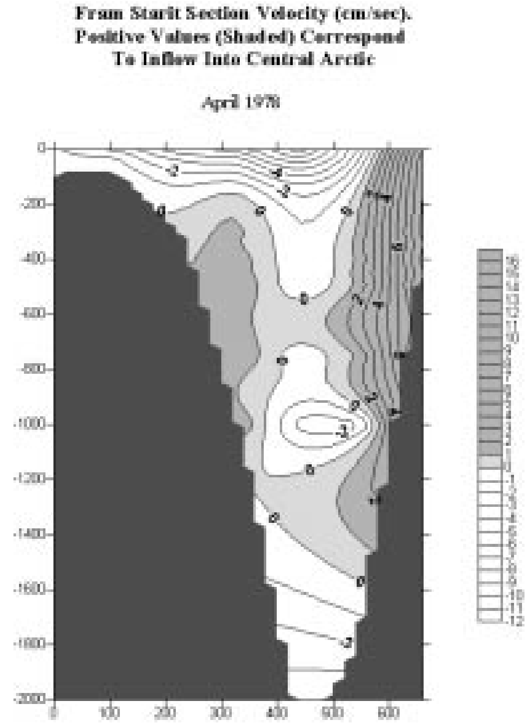

Fig. 7. Fram Strait Section. Velocity (cm/s). Greenland is to the left.

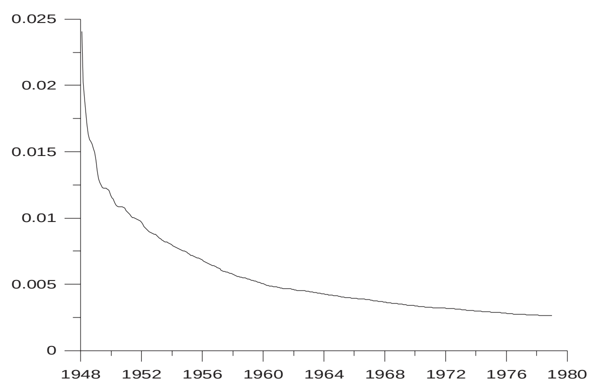

Fig. 8. Time series of the mean temperature (grad C) in the layer 450-1500m

approximately 20 years. This time scale may be correlated with the dissipative cooling of the AW layer (see Fig. 8).

During both winter and summer the average ice compactness was approximately 0.8-0.83. According to observations (Chapman and Walsh, 1993) the winter average compactness should be about 0.9 .

The April and September monthly means of ice thickness and ice drift velocities are shown on Figs. 11 and 12. The general structure is quite realistic, with the maximum ice thickness about 7 m at Canadian Archipelago. Mean ice thickness is 335 and 295 cm for April and September, and the corresponding ice thickness at North Pole is 355 and 305 cm. The scheme of ice drift is also realistic with the pronounced Transpolar Drift.

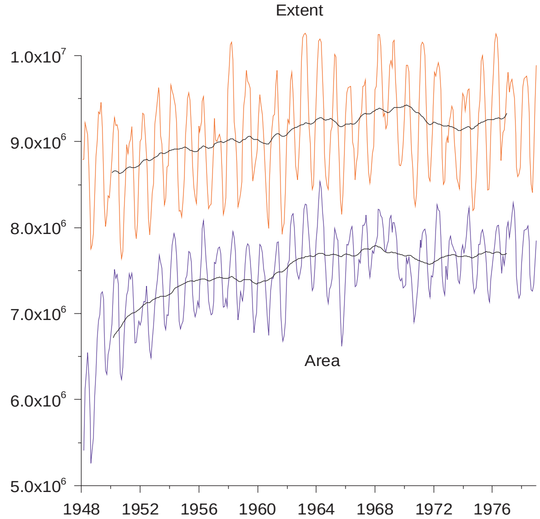

Fig. 9. Time series of ice area (blue) and ice extent (red) for 31-year spin-up (km^2). Black lines are 4-years running averages.

The discrepancy of model results and observations (Chapman and Walsh, 1993) may be shown in more details for the year 1978 (Fig. 10). The drawback is the too extended ice coverage in Barents Sea, especially during summer. According to observations all the Barents Sea and southern half of the Kara Sea were open on September 1978. This feature is supposed to be due to the weak Atlantic Water inflow in Barents Sea by North Cape current. The other possible reason for this process is the cooling of the warm AW. Also, one may note the weak wind-driven component of sea ice drift because of small wind drag coefficient. AOMIP specification is

$$C_D = (1.1 + 0.04 \cdot W) \cdot 10^{-3}, \qquad (15)$$

W is wind velocity in m/s. These values are in contrast with the SIMIP (Kreyshner M., 2000) estimates of $C_D = 2.75 \cdot 10^{-3}$, derived on the basis of buoy drift statistics (Colony and Rigor, 1995). In a case of higher C_D one may expect more open water in Barents-Kara region (note the direction of monthly mean ice drift). Indeed, in some test runs with the higher C_D the ice cover area tends to be smaller.

Comparison with the snow depth data (EWG, 2000) shows that snow thickness (Fig. 13) is of the same scale 30-40 cm, although in contrast with the data the maximum is shifted from the Greenland area to the northern Barents Sea.

5. SUMMARY

The presented “toy” coarse resolution model was developed primarily to test numerical methods and physical parameterizations. Some of the results look quite acceptable even in comparison with

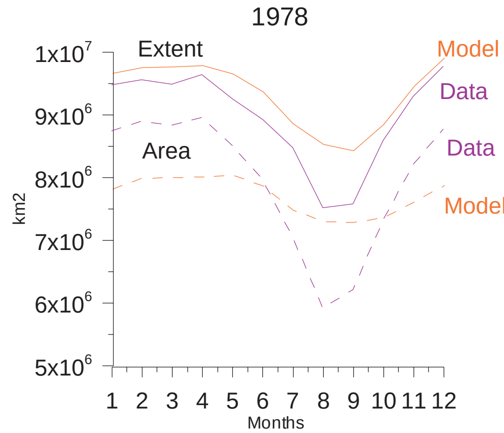

Fig. 10. Modeled ice area and ice extent (red) in comparison with the observations(violet) during the year 1978. Ice extent presented by solid line and area – by dashed.

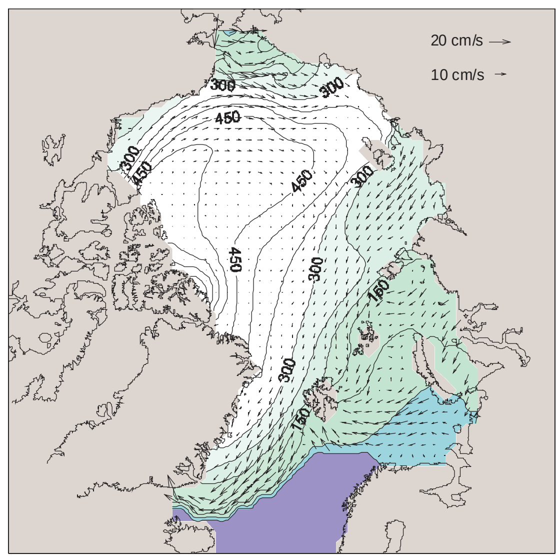

Fig. 11. Sea ice thickness (cm) and ice drift velocities for April 1978.

higher resolution models. Despite the drawbacks (explained mainly by the resolution and inevitable overestimated diffusivity and viscosity) model describes all the large-scale features of the Arctic Ocean water-ice system. The presented model is a good basis for the further development, investigations of the key processes of Arctic Ocean climate variability and testing the new parameterizations and numerical schemes.

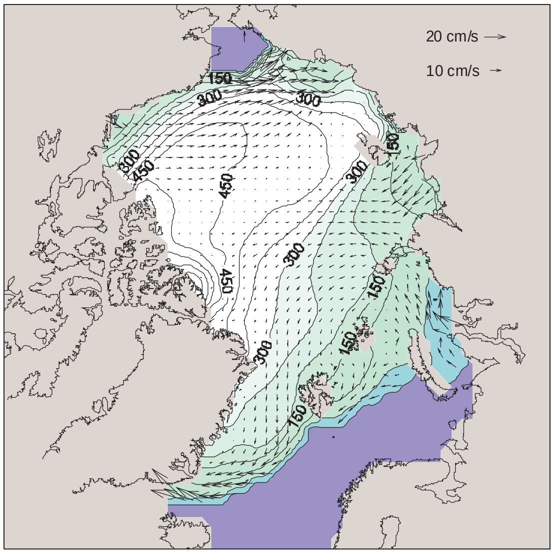

Fig. 12. Sea ice thickness (cm) and ice drift velocities for September 1978.

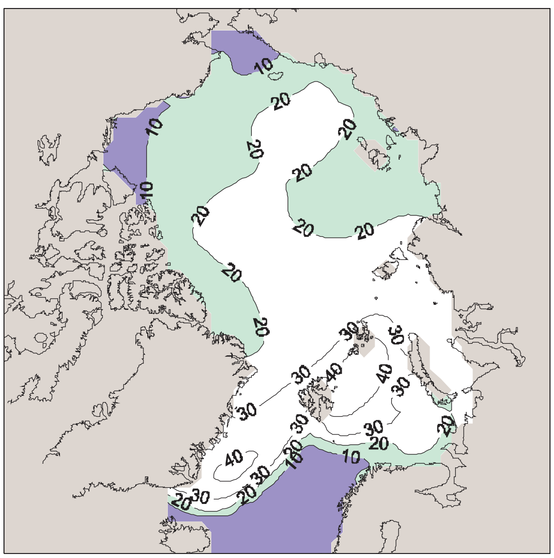

Fig. 13. Snow thickness (cm) for April 1978.

Acknowledgment

The work was done in the frame of the Arctic Ocean Intercomparison Project (AOMIP). The author has a travel support by Internatinal Arctic Research Center (IARC, Uni. Alaska Fairbanks, AK) and NSF through WHOI AOMIP project.

References

Blumberg, A.F., and G.L. Mellor, 1987: A description of a three-dimensional coastal ocean circulation model. In: *Three-Dimensional Coastal Ocean Models,* Coastal and Estuarine Series, ed. Moores, **4**, 1-16.

Bryan, K.H., 1969: A numerical method for study of the circulation of the World Ocean. *J. Comp. Phys.*, **4**, 347-376.

Chapman, W., and J. Walsh, 1993: Recent variations of sea ice and air temperature in high latitudes. *Bull. AMS*, **74**, No1.

Colony, R., and I. Rigor, 1995: Arctic ocean buoy data program report. *Appl. Phys. Lab. Tech. Memo. APL-UW TM 10-91.* Nat. Snow and Ice Data Cent. (NSIDC), Boulder, Colo.

Cox, M.D., 1984: A primitive equation three-dimensional model of the ocean. *Tech Report*, **1**, GFDL Ocean Group, Princeton University.

Ebert, E. E., and J.A. Curry, 1993: An intermediate one-dimensional thermodynamical sea ice model for investigating ice-atmosphere interactions. *J. Geophys. Res.*, **98**, 10,085-10,109.

Environmental Working Group (EWG), 2000: Joint U.S. - Russian Arctic Atlas: The Arctic Climatology Project: Arctic Meteorology and Climate Atlas [CD-ROM]. Natl. Snow and Ice Data Center, Boulder, Colorado.

Harder, M., 1996: Dynamik, Rauhigkeit und Alter des Meereises in der Arktis. PhD thesis, Alfred-Wegner-Institut fur Polar-ind Meeresforschung, Bremerhaven, Germany.

Hibler, W. D., 1979: A dynamic thermodynamic sea-ice model, *J. Phys. Oceanogr.*, **9**, 815-846.

Hibler, W. D., and K. Bryan, 1987: A diagnostic ice-ocean model. *J. Phys. Oceanogr.*, **17**, 987-1015.

Holloway, G., 1992: Representing topographic stress for large–scale ocean models. *J. Phys. Oceanogr.*, **22**, 1033-1046.

Hughes, T.J.R. and A. Brooks, 1979: A multi-dimensional upwind scheme with no crosswind diffusion. In: T.J.R. Hughes, Ed., Finite Element Method for Convection Dominated Flows. AMD, **34**, 19-35. ASME, NY.

Hushchke, R. E., 1969: Arctic cloud statistics from 'air-calibrated' surface weather observations. *Memo. RM-6173-PR*, Rand Corp., Santa Monica, Calif., 79 pp.

Iakovlev, N.G., 1998: Numerical model of the general circulation of the Arctic ocean. A new version and preliminary calculation results. *Russ. J. Numer. Anal. Math. Modelling*, **3**, No 6, 465-478.

Kazantsev E., J. Sommeria, and J. Verron, 1998: Subgrid-Scale eddy parametrization by statistical mechanics in a barotropic ocean model. *J. Phys. Oceanogr.*, **28**, N 6, 1017-1042.

Kowalik, Z., and I. Polyakov, 1999: Duirnal tides over Kashevarov Bank, Okhotsk Sea. *J. Geophys. Res.*, **104**, No C3, 5361-5380.

Kreyshner M., M.Harder, P.Lemke and G.Flato. 2000: Results of the Sea Ice Model Intercomparison Project: Evaluation of sea ice rheology schemes for use in climate simulations. *J. Geophys. Res.*, **105**, No C5, 11299-11320.

Maslowski W., 1996: Numerical simulation of topographic Rossby waves along the East Greenland front. *J. Geophys. Res.*, **101**, No C4, 8775-8787.

Millero, F.J., 1978: Freezing point of sea water. 8th Report of the Joint Panel on Oceanographic Tables and Standards, UNESCO Tech. Pap. In Mar. Sci., **28,** Annex 6, 29-35, UNESCO, Paris.

Nazarenko, L., G. Holloway and N. Tausnev, 1998: Dynamics of transport of 'Atlantic signature' in the Arctic Ocean. *J. Geophys. Res.*, **103**, No C13, 31003-31015.

Parkinson, C.L. and W.M. Washington, 1979: A large scale numerical model of sea ice. *J. Geophys. Res.*, **84**, 311-337.

Polyakov, I., 2001: An eddy parameterization based on maximum entropy production with application to modeling of the Arctic Ocean circulation. *J. Phys. Oceanogr.,* **31**, 2255-2270.

Steele, M., R.Morley, and W. Ermold, 2001: PHC: A global ocean topography with a high quality Arctic Ocean. *J. Climate,* **14**, 2079-2087.

Wadhams, P., A.E. Gill, and P.F. Linden, 1979: Transects by submarine of the East Greenland front. *Deep Sea Res.*, **26**, 1311-1328.

Weatherly, J.W. and J.E. Walsh, 1996: The effects of precipitation and river runoff in a coupled ice-ocean model of the Arctic. *Clim. Dyn.*,. 12. 785-798.

Yang, D., 1999: An improved precipitation climatology for the Arctic Ocean, *Geophys. Res. Lett.*, **26**(11), 1625-1628.

Zhang, J., D.A. Rothrock, and M. Steele, 1998: Warming of the Arctic Ocean by a strengthened Atlantic inflow: Model results. *Geophys. Res. Lett.*, **25**, 1745-1748.